Geochemistry of Lavas from Mauritius, Indian Ocean: Mantle Sources and Petrogenesis

H. C. SHETH,[1] J. J. MAHONEY,

Department of Geology and Geophysics, School of Ocean and Earth Science and Technology (SOEST),
University of Hawaii at Manoa, Honolulu, Hawaii 96822

AND A. N. BAXTER

School of Earth and Environmental Sciences, University of Greenwich, Chatham Maritime, Kent, ME4 4TB United Kingdom

Abstract

Trace-element and Nd-Sr-Pb isotopic data for mafic lavas from the Mascarene island of Mauritius reveal that the shield-stage Older Series (with $^{143}Nd/^{144}Nd$ = 0.512827 to 0.512853, $^{87}Sr/^{86}Sr$ = 0.70412 to 0.70433, and $^{206}Pb/^{204}Pb$ = 18.771 to 19.024) is geochemically very similar to the shield-building lavas of the younger island of Réunion. The post-shield Intermediate and Younger Series lavas of Mauritius have systematically greater values of $^{143}Nd/^{144}Nd$ and lower $^{87}Sr/^{86}Sr$ ratios than the Older Series and Réunion lavas. Intermediate and Younger Series Nd and Sr isotopic ratios are closely similar (0.512874 to 0.512899; 0.70369 to 0.70401), whereas $^{206}Pb/^{204}Pb$ ranges from values as great as any for the Older Series and Réunion lavas to as low as 18.608. Most of the Intermediate Series lavas are strongly enriched in highly incompatible elements relative to moderately incompatible ones (e.g., chondrite-normalized La/Lu = 4.03–17.8 vs. 9.38–10.2 for the Older Series), but the Younger Series lavas display much less relative enrichment (e.g., chondrite-normalized La/Lu = 3.86–5.37) and have low concentrations of incompatible elements. Modeling suggests that variable partial melting and mixing between mid-ocean–ridge–basalt (MORB) source mantle and mantle with bulk-Earth–like Nd and Sr isotopic and incompatible-element ratios, and "C"-like Pb isotope ratios, can explain the general relationship between the shield and post-shield lavas. All Mauritius and Réunion lavas can be explained as 2–8% partial melts of a bulk-Earth–like source that had been 1.5–0.25% metasomatized by a 0.1% MORB-source melt. The range in Pb isotopic compositions requires mixing with highly variable Sr/Pb and Nd/Pb ratios in the end members; such variation, however, is not supported by measured Sr/Pb, Nd/Pb, etc. in the lavas. Some isotopic heterogeneity thus appears to be required in the end members and/or much of the range in Pb isotopes represents radiogenic ingrowth since the metasomatic event. Near-constant $^{207}Pb/^{204}Pb$ values over the range of $^{206}Pb/^{204}Pb$ among the Older Series lavas suggest that the metasomatic event must have occurred within the last few hundred million years.

Introduction

THE INDIAN OCEAN BASIN has a complex geology, with four major branches of the worldwide oceanic ridge system (the Southeast Indian, Southwest Indian, Central Indian, and Carlsberg ridges), numerous large fracture zones, and several volcanic island/seamount chains (Fig. 1). The island of Mauritius (20°20'S, 57°30'E) lies at the southern end of the Mascarene Plateau, a major volcanic edifice that extends northward to the Seychelles Islands (e.g.,

Fisher et al., 1967, 1971; Baxter, 1975a, 1975b). The islands of Mauritius, Rodrigues (650 km ENE of Mauritius), and Réunion (170 km WSW of Mauritius) together constitute the Mascarene Islands.

Volcanic activity on Rodrigues ceased ~1.5 Ma (million years ago), and that on Mauritius at 0.17 Ma (McDougall and Chamalaun, 1969), whereas Réunion Island is still volcanically active. Morgan (e.g., 1981) proposed that the Réunion "hotspot" was the manifestation of a deep mantle plume, and that the track of this plume on the northward-moving Indian plate is represented by Réunion, Mauritius, and the Mascarene Plateau, the Laccadives-Maldives-Chagos Ridge, and the Deccan flood basalt province of India (Fig. 1). Morgan (1981) also specu-

[1]Corresponding author; email: hcsheth@iitb.ac.in. Now at Department of Earth Sciences, Indian Institute of Technology (IIT), Powai, Bombay 400076 India.
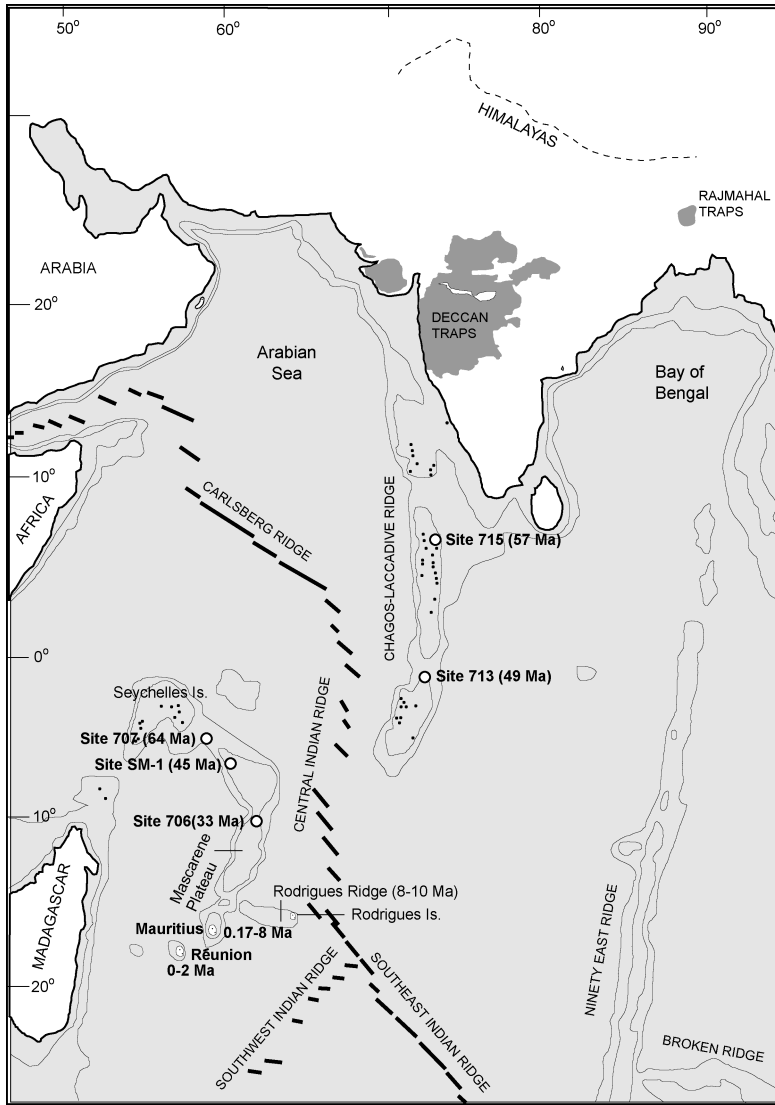
FIG. 1. Map of southern Asia and the Indian Ocean basin, showing the main tectonic and physiographic features of the latter. Based on maps of Mahoney et al. (2002) and Duncan (1990). ODP Leg 115 sites (706, 107, 713, 715) and Texaco drill site SM-1 are indicated by open circles; the ages of the basalts are from McDougall and Chamalaun (1969) and Duncan and Hargraves (1990).

lated that the E-W–trending Rodrigues Ridge formed by lateral flow of Réunion hotspot mantle toward the Central Indian Ridge (CIR), as the CIR gradually migrated away from the hotspot. The Rodrigues Ridge does not extend all the way to the CIR, however, and appears to lack an age progression (Duncan, 1990); Rodrigues Island lies at its eastern terminus.

Réunion Island rises 7 km from an ocean floor of Paleocene age and consists of two shield volcanoes. Piton de La Fournaise (2,361 m) is active, and one of the most productive in the world. The other, Piton des Neiges (3,069 m), lies 30 km northwest of Piton de la Fournaise, and is now extinct (Bachèlery et al., 1982; Fisk et al., 1988). Lavas from both volcanoes

have been studied extensively (e.g., McDougall, 1971; Fisk et al., 1988; Albarède and Tamagnan, 1988; Gillot and Nativel, 1989; Staudacher et al., 1990; White et al., 1990; Albarède et al., 1997; Hanyu et al., 2001). In comparison, few studies of Rodrigues Island lavas exist (e.g., McDougall et al, 1965; Baxter et al., 1985). For Mauritius, K-Ar (McDougall and Chamalaun, 1969), petrographic, major-element and some trace-element data (Baxter, 1972; 1975a, 1975b, 1976) are available, along with a small number of isotopic data. The latter include Nd and Sr isotopic data for eight samples (Mahoney et al., 1989), and Pb isotopic data for two of these samples (Peng and Mahoney, 1995). Noble gas isotope data for a few Mauritius lavas and for a larger number of Réunion lavas were recently published by Hanyu et al. (2001). In this paper, we present major-element, detailed trace element, and Nd-Sr-Pb isotopic data for a suite of Mauritius lavas, and discuss the implications for the mantle sources and petrogenetic evolution of these lavas.

General Volcanic Geology of Mauritius

Baxter (1972) recognized three distinct volcanic series on Mauritius: the Older, Intermediate, and Younger Series. The Older Series, marking the erosional remnants of a large shield volcano, is a variably differentiated transitional basalt to trachyte suite (Baxter, 1975a). It is composed of two stages. The first, a shield-building stage, consists of an alternating lava-agglomerate succession with flows of olivine basalt, with minor feldspar-phyric basalt and trachybasalt toward the top of the succession; the porphyritic mafic lavas host ultramafic nodules. A radial dike swarm is associated with this stage. The second stage forms a late-shield sequence of feldspar-phyric basalt and trachybasalt, with associated trachytic intrusions. The post-shield Intermediate Series lavas are restricted to the southwestern part of the island, and predominantly comprise alkali-olivine basalt, basanite, and subordinate nephelinite. The volume of the Intermediate Series is small compared to the volumes of the Older and the Younger Series. Younger Series lavas cover the bulk of the island, and are mostly olivine basalts with smaller volumes of basanite. They were probably erupted as the terminal stages of major fissure eruptions from a group of small volcanoes aligned ENE-WSW. K-Ar dating by McDougall and Chamalaun (1969) yielded ages of 7.8–5.5 Ma for the Older Series, 3.5–1.9 Ma for the Intermediate Series, and 0.70–0.17 Ma for the Younger Series.

The evolution of Mauritius is rather similar to that of many ocean islands worldwide, including the Hawaiian islands. Hawaiian volcanoes typically evolve through four distinct eruptive stages (e.g., Stearns, 1940; Macdonald and Katsura, 1964; Macdonald, 1968; Clague, 1987). The first is a pre-shield stage, consisting of alkalic and some tholeiitic lavas, followed by a tholeiitic shield-building stage that constitutes ~99% of a volcano's volume. This is followed by a post-shield alkalic stage, and often, several million years later, a post-erosional or rejuvenated alkalic stage. The pre-shield stage has been observed only for the youngest volcano in the Hawaiian chain, Loihi, and is inferred for the other Hawaiian volcanoes whose inaccessible foundations lie several kilometers underneath their exposed tops.

Using the major elements and several trace elements, Baxter (1975a) inferred an important role for fractionation of olivine + clinopyroxene (± plagioclase ± titanomagnetite) in the evolution of the Mauritius Older Series basalts, and the fractionation of anorthoclase in the evolution of the trachytes. He tentatively ascribed a distinct "silica gap" within the series to secondary boiling. Baxter (1976) argued that incompatible-element enrichment patterns in alkali basalts from the Intermediate and Younger Series, and their highly variable Rb/Sr, K/Rb, K/Sr, and K/Ba ratios, suggested formation by low-degree, possibly sequential melting of a single peridotitic mantle source. He suggested that the relatively low incompatible-element concentrations in the Younger Series either reflected higher degrees of partial melting, or the melting of mantle already depleted in incompatible elements during production of the Intermediate Series magmas.

Samples and Analytical Methods

The samples used in this study are from Baxter's collection, and all are from lava flows. Major element oxides (except Na_2O) and several trace elements in a large number of tungsten-carbide-ground powders were analyzed by Baxter (1972) using X-ray fluorescence spectrometry (XRFS); Na_2O was analyzed by flame photometry. We analyzed fourteen of these samples for a larger suite of trace elements, including the lanthanide rare-earth elements (REE), at the University of Hawaii by inductively coupled plasma mass spectrometry (ICPMS), following the method of Jain and Neal (1996). Major- and trace-element compositions are reported in Table 1. Nine of the samples (three from each series) were also analyzed for Nd, Sr, and Pb isotopic ratios, and Pb

TABLE 1. Major- and Trace-Element Compositions of Mauritius Lavas[1]

Series:	OS	OS	OS	IS	IS	IS	IS	IS	IS	YS	YS	YS	YS	YS	Recomm.	Meas.
Type:	SAB	SAB	AB	AB	BAS	AB	AB	BAS	BAS	AB	AB	AB	SAB	AB		
Sample:	A168	A169	A215	B1	B5	B18	B19	B33	B34	C4	C20	C29	C52	C60	AGV-1	AGV-1
SiO_2	47.31	47.31	45.86	45.80	44.13	46.28	45.58	43.54	42.80	45.93	46.19	46.48	45.18	46.26	59.25	59.07
TiO_2	2.66	2.66	2.93	1.65	2.34	1.77	1.91	2.36	2.71	2.06	1.73	1.83	1.94	1.99	1.06	1.06
Al_2O_3	13.55	13.03	13.76	14.21	13.02	14.10	13.74	12.29	12.12	15.64	15.02	15.70	14.55	16.08	17.15	17.30
Fe_2O_3	1.55	4.25	3.90	2.77	2.24	1.74	1.86	6.54	3.80	2.52	1.42	1.39	3.03	1.81	4.47	***[2]
FeO	10.45	7.83	8.32	10.71	8.97	10.35	10.88	5.74	8.82	9.73	10.49	10.13	9.36	10.65	2.06	***
MnO	0.15	0.16	0.15	0.21	0.16	0.16	0.19	0.18	0.18	0.15	0.17	0.16	0.17	0.17	0.10	n.a.
MgO	9.73	9.60	9.13	10.41	10.64	10.39	10.69	13.12	12.58	8.24	9.62	8.35	10.44	7.90	1.53	1.45
CaO	9.87	9.61	10.12	9.99	12.08	10.58	10.42	11.30	11.09	10.44	11.31	11.62	11.07	10.48	4.94	4.99
Na_2O	2.92	2.82	2.65	2.85	3.09	2.58	2.96	3.26	2.60	3.38	2.88	2.87	2.30	3.10	4.25	n.a.
K_2O	1.02	1.01	0.94	0.34	1.15	0.40	0.63	0.76	1.33	0.58	0.29	0.33	0.16	0.40	2.90	2.88
P_2O_5	0.42	0.46	0.34	0.24	0.43	0.24	0.28	0.43	0.51	0.27	0.16	0.21	0.16	0.20	0.48	0.45
H_2O^+	0.33	0.88	1.38	1.58	0.64	0.57	0.62	0.88	1.61	0.26	0.26	0.46	1.43	0.81		
Total	99.96	99.62	99.48	100.76	98.89	99.16	99.76	100.40	100.15	99.20	99.54	99.53	99.79	99.85		
Mg No.	62.4	68.6	66.2	63.4	67.9	64.1	63.6	80.3	71.8	60.1	62.0	59.5	66.5	56.9	BHVO-1	BHVO-1
Ni	352	390	253	425	335	277	361	448	427	163	258	149	355	175	121	n.a.
Cr	349	408	317	361	360	402	378	431	367	109	329	237	346	50	289	n.a.
V	263	284	338	229	253	200	241	283	296	190	256	261	242	261	317	n.a.
Rb	31	34	24	9	42	11	22	13	46	17	12	4	5	7	9.7	n.a.
Ba	268	301	238	171	491	207	238	524	571	195	106	137	189	150	133	136
Th	2.91	3.13	2.49	0.81	3.37	0.34	1.89	3.50	3.97	1.82	1.09	0.92	1.40	1.35	1.08	1.11
U	0.86	0.84	0.38	0.22	0.92	0.08	0.52	0.97	1.18	0.49	0.27	0.18	0.11	0.29	0.42	0.42
Nb	32	32	32	13	49	24	23	45	54	22	12	14	17	17	19	22
Ta	1.9	1.9	1.9	0.73	2.7	1.7	1.3	2.5	3.0	1.4	0.70	1.0	1.3	0.98	1.16	1.3
La	26.5	27.4	25.3	10.5	33.2	n.a.	17.1	32.2	39.9	14.5	9.02	9.74	12.8	14.0	15.8	18.2
Ce	53.4	55.1	52.0	22.1	59.3	n.a.	32.8	61.7	76.2	29.9	18.9	20.6	26.6	24.2	38.0	41.7
Pr	7	7.19	6.88	3.25	7.54	n.a.	4.56	7.87	9.51	4.18	2.75	3.06	3.79	3.59	5.70	6.25
Pb	2.0	2.1	1.9	1.3	2.5	1.9	1.2	2.3	2.6	1.2	0.7	0.9	2.0	0.9	2.05	2.20
Sr	418	397	380	281	545	276	346	520	595	391	326	326	362	327	403	n.a.
Nd	29.5	30.2	29.3	14.5	30.9	n.a.	19.4	32.1	38.9	18.0	12.4	13.8	16.5	16.1	25.2	28.5
Zr	210	215	203	107	162	n.a.	114	170	214	124	80	88	102	106	179	192
Hf	5.14	5.16	5.04	2.62	4.03	n.a.	3.04	4.14	5.04	3.16	2.19	2.29	2.66	2.73	4.38	4.94
Sm	6.64	6.69	6.72	3.86	6.63	n.a.	4.84	6.88	8.16	4.59	3.35	3.77	4.18	4.14	6.20	7.09
Eu	2.17	2.17	2.20	1.41	2.21	n.a.	1.66	2.25	2.63	1.63	1.27	1.37	1.52	1.48	2.06	2.16
Gd	6.74	6.79	6.82	4.46	6.76	n.a.	5.40	6.82	7.94	5.09	3.98	4.34	4.72	4.78	6.40	7.72
Tb	1.00	1.01	1.03	0.72	0.97	n.a.	0.85	1.00	1.14	0.82	0.66	0.71	0.74	0.78	0.96	1.12
Dy	5.37	5.47	5.50	4.36	5.06	n.a.	4.85	5.14	5.63	4.65	4.02	4.29	4.40	4.61	5.20	6.18
Y	29.0	29.5	29.3	23.6	29.1	n.a.	25.3	26.2	28.4	23.9	21.0	22.2	22.2	26.7	27.6	31.9
Ho	1.03	1.02	1.04	0.84	0.92	n.a.	0.95	0.94	1.00	0.91	0.81	0.85	0.85	0.91	0.99	1.16
Er	2.48	2.48	2.49	2.11	2.10	n.a.	2.32	2.21	2.30	2.23	2.01	2.09	2.05	2.28	2.40	2.76
Tm	0.33	0.34	0.34	0.29	0.28	n.a.	0.33	0.29	0.29	0.31	0.28	0.29	0.28	0.32	0.33	0.38
Yb	2.04	2.07	2.02	1.85	1.62	n.a.	2.05	1.77	1.77	1.96	1.76	1.83	1.78	1.99	2.02	2.30
Lu	0.29	0.29	0.29	0.28	0.23	n.a.	0.30	0.25	0.24	0.29	0.25	0.27	0.26	0.29	0.29	0.33

[1]The rock series are OS (Older), IS (Intermediate), and YS (Younger). The rock names (obtained using the SINCLAS program of Verma et al. (2002) are alkalic basalt (AB), subalkalic basalt (SAB), and basanite (BAS). Major-element data are in weight percent (wt%); trace elements are in parts per million (ppm). Major-element and Rb, Ba, Sr, Ni, Cr, and V data were obtained by XRFS, except Na_2O, which was measured by flame photometry. For the major-element data, an indication of accuracy is given by measured and recommended values (from Potts et al., 1992) for standard rock AGV-1.

[2]The symbol "***" indicates that, for the samples, total Fe was measured by XRFS, and FeO by the ammonium vanadate titration method; Fe_2O_3 was calculated from the difference. For AGV-1, the measured value of total Fe as FeO was 6.27 wt% and the recommended value (Potts et al., 1992) is 6.08 wt%. For the ICPMS data, accuracy is indicated by the measured and recommended values (mostly from Govindaraju, 1989) for standard rock BHVO-1. For trace elements at >0.4 ppm in the rock and analyzed by ICPMS, the relative uncertainty for most elements is 3.5% or better (range is 1–5%). Percentage precision for the XRFS data is as follows: $SiO_2 = 0.55$, $TiO_2 = 1.94$, $Al_2O_3 = 1.02$, FeO total = 1.76, MnO = 3.80, MgO = 1.96, CaO = 0.54, $K_2O = 0.43$, $P_2O_5 = 3.80$, Ni = 4, Cr = 12, V = 5, Rb = 7, Ba = 6. Percentage precision on Na_2O is 0.90; n.a. = not analyzed/available.

TABLE 2. Isotopic and Pb Isotope Dilution Data for Mauritius Lavas

Sample:	A168	A169	A215	B5	B18	B33	B34	C20	C29	C52
$^{143}Nd/^{144}Nd$	0.512841	0.512842	0.512853	0.512875	0.512897	0.512895 (0.000014)	0.512899	0.512874	0.512882	0.512891
ε_{Nd}	+3.9	+3.9	+4.1	+4.6	+5.0	+5.0 0.3	+5.0	+4.6	+4.7	+4.9
$^{87}Sr/^{86}Sr$	0.70429	0.70431	0.70412	0.70372	0.70381	0.70384 (0.00003)	0.70379	0.70401	0.70376	0.70377
Pb (ppm)	2.18	2.45	2.15	2.58	1.06		2.15	0.78	0.91	0.89
$^{206}Pb/^{204}Pb$	18.940	18.770	19.024	19.004	18.974	na	18.634 (0.005)	18.688	18.617 (0.005)	18.608
$^{207}Pb/^{204}Pb$	15.595	15.596	15.609	15.598	15.595	na	15.569 (0.005)	15.569	15.580 (0.005)	15.571
$^{208}Pb/^{204}Pb$	39.024	38.843	39.113	39.133	39.088	na	38.633 (0.010)	38.713	38.635 (0.010)	38.617

[2]All isotopic ratios are present-day values. ε_{Nd} = 0 today corresponds to $^{143}Nd/^{144}Nd$ = 0.512640. Nd and Sr isotope data for sample B33 are from Mahoney et al. (1989). Data are reported relative to values of $^{87}Sr/^{86}Sr$ = 0.71024 for NBS 987 Sr and $^{143}Nd/^{144}Nd$ = 0.511845 for La Jolla Nd. For Pb isotopes, the total range on ~5 ng loads of NBS 981 in the 2000-2002 period was ~250 ppm for each ratio for double-spike measurements, and the mean ratios measured are 16.937, 15.492, and 36.710. The total range measured for NBS 987 Sr over this period was ± 0.000020; for La Jolla Nd it was ± 0.0000010 (0.2 ε_{Nd} units). Within-run errors on the isotopic data above are less than or equal to the external uncertainties on these standards, except as shown in parentheses.

abundance by isotope dilution, at the University of Hawaii following the methods of Mahoney et al. (1991), except that Pb isotope measurements employed a double-spike method (Galer, 1999). The isotopic data are presented in Table 2; because of the young ages of all three series, the data are not age-corrected.

Major and Trace Elements

We used the SINCLAS program (Verma et al., 2002) to calculate normative compositions and Mg numbers (Mg#), and to obtain rock names. Three of our samples are classified as subalkalic basalts (Older Series samples A168 and A169, and Younger Series lava C52); these three have normative hypersthene. Eight samples are alkalic basalts; they lack normative hypersthene but contain normative nepheline. Three others (B5, B33 and B34), all from the Intermediate Series, are classified as basanites, with ~9–11% normative nepheline, low SiO_2 contents (<45 wt%), and relatively high MgO (11–12 wt%). Data for all the samples analyzed by Baxter (1972) are plotted in the total alkalis-silica diagram of Le Bas et al. (1986) in Figure 2. The heavy curve is the boundary between the subalkalic and alkalic fields as proposed by Irvine and Baragar (1971). The majority of the data lie in the alkalic basalt field. Several high-MgO samples lie in the picrobasalt and tephrite-basanite fields. MgO contents and Mg# (= [atomic $Mg/(Mg + Fe^{2+})$] x 100, assuming Fe^{3+}/Fe^{2+} = 0.16) are quite high for most of the samples we analyzed; i.e., most of our rocks are rather primitive. The lowest value for Mg# is 56.9 (sample C60), and the two highest values are 80.3 (B33) and 71.8 (B34). Baxter (1975a) interpreted several high-MgO lavas of the Older Series as having accumulated olivine, and concluded (Baxter, 1976) that many high-MgO lavas of the Intermediate Series represent primitive, near-primary liquids.

Figure 3 shows primitive mantle–normalized element patterns for the Mauritius lavas along with the pattern for average Réunion shield-stage tholeiite for comparison. Patterns for the Older Series lavas
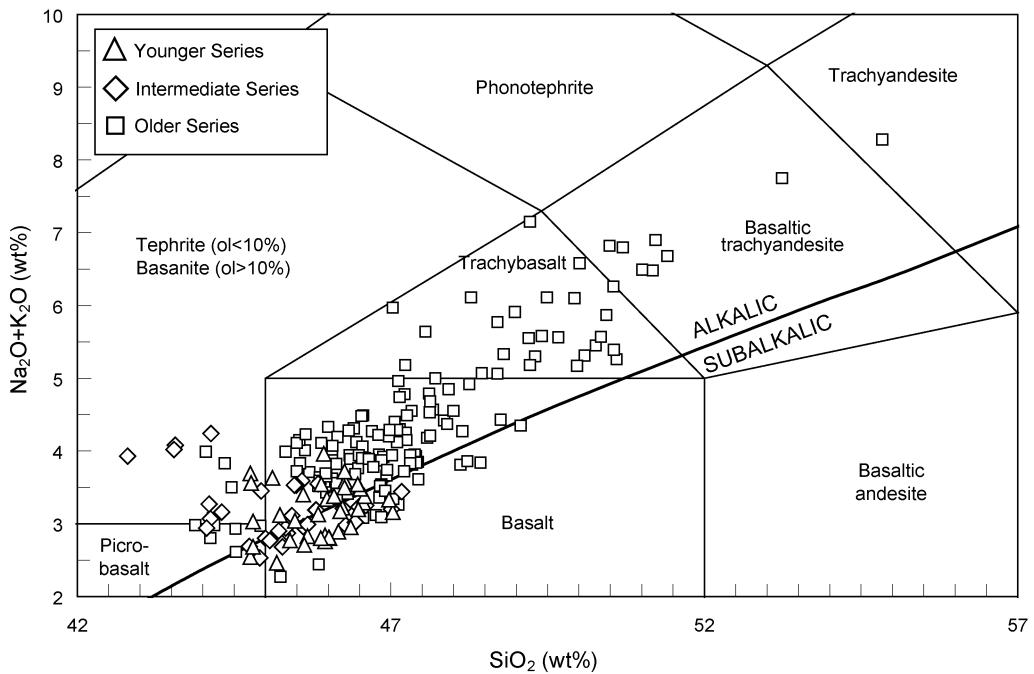
FIG. 2. Data for Mauritius lavas plotted on the total alkalis-silica (TAS) diagram of Le Bas et al. (1986). Abbreviations: ol = normative olivine. Trachytes and trachydacites of the Older Series are not shown.

show small Pb and Nb-Ta peaks, with small troughs at Sr and, in one case, P (Fig. 3A). Their strong similarity to the average Réunion pattern is evident, although the Older Series lavas exhibit slightly greater relative enrichment in the highly incompatible elements. The small U peak in the Réunion pattern is also present in the patterns for A168 and A169. However, sample A215 shows a trough at U, probably a result of U loss caused by alteration (its H_2O content is 1.38%; Table 1).

Baxter (1976) suggested, based on petrographic and chemical data, that most of the Intermediate Series lavas, comprising alkalic basalts, basanites, and nephelinites, were primitive mafic liquids erupted almost unmodified from upper mantle levels, possibly 45–60 km. We did not analyze any Intermediate Series nephelinites, but the alkalic basalt and basanite patterns display a substantial range in slope. Alkalic basalt B19 has a pattern rather similar in overall slope to the average Réunion shield pattern, but that for B1 is much flatter. Both the B1 and B19 patterns have peaks at Nb-Ta, like the Older Series and Réunion patterns (Fig. 3B). However, whereas B1 shows a Pb peak, B19

lacks one, and B19, in particular, is poor in Zr and Hf relative to Nd or Sm. Also, Ba in sample B1 is high relative to Rb and Th; this may reflect some post-eruptive redistribution of Rb and/or Ba, or it may be a primary feature because the basanites (Fig. 3C) also have high relative Ba abundances. The most prominent feature of the basanite patterns is their steepness relative to those for the alkalic basalts, the Older Series, and Réunion shield lavas. The basanite patterns also have pronounced Nb-Ta peaks, small but distinct Pb and U peaks, and slight troughs at Zr-Hf. Sample B33 seems to have lost some Rb and K as a result of alteration (its H_2O content is 0.88%). The variable enrichment in the light REE over the heavy REE, and the crossing REE patterns, are suggestive of small but variable extents of partial melting with, at least in some cases, residual garnet in the source (La/Yb = 18.19 to 22.54). This feature is consistent with formation of some of these magmas at depths greater than about 80 km (e.g., O'Hara et al., 1971).

Patterns of the Younger Series lavas (Figs. 3D and 3E) contrast strongly with the steeper ones of the Older Series basalts and especially the
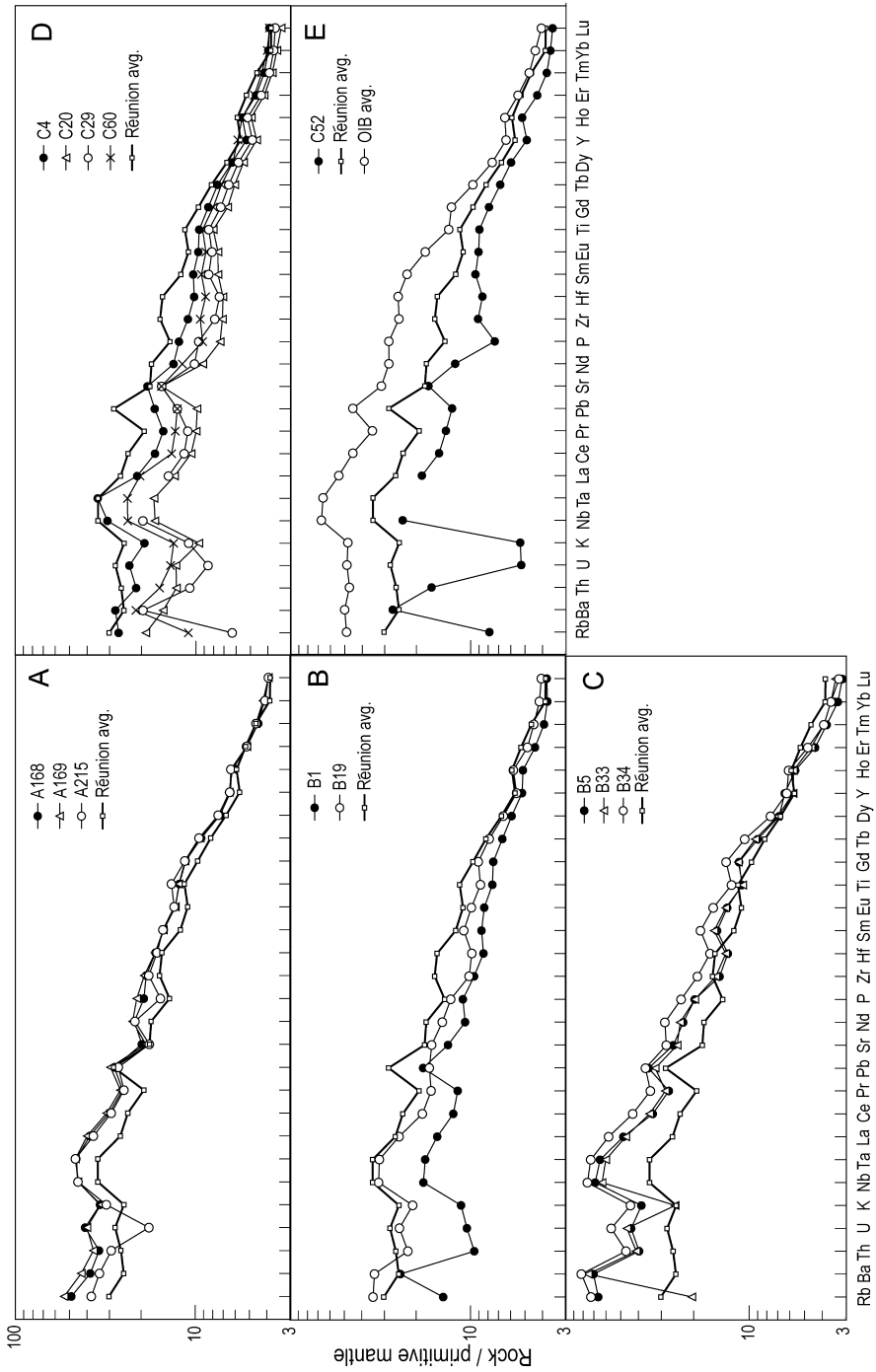
FIG. 3. Primitive mantle–normalized element patterns for Mauritius lavas. Normalizing values and global average OIB (ocean island basalt) pattern in panel E are from Sun and McDonough (1989). Average Réunion pattern (data from Fisk et al., 1988; Albarède et al., 1997) is shown for comparison.
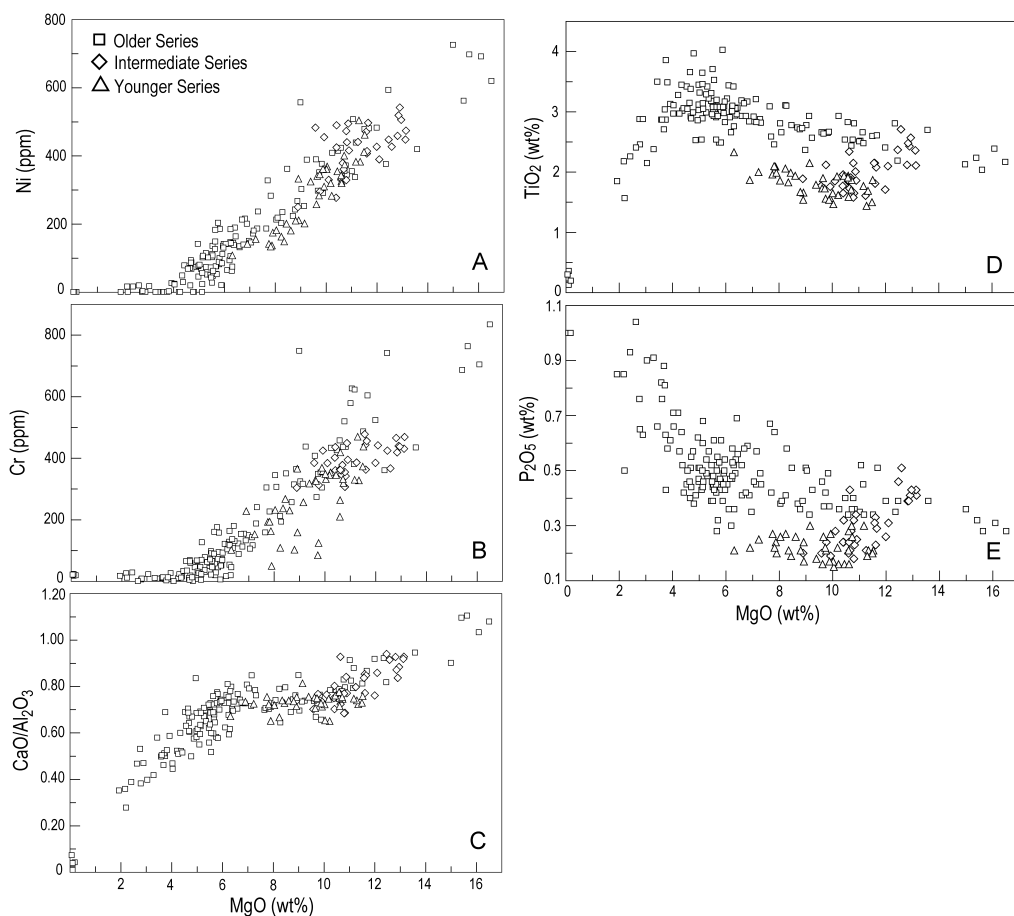
FIG. 4. The variation of MgO with (A) Ni, (B) Cr, (C) CaO/Al$_2$O$_3$, (D) TiO$_2$, and (E) P$_2$O$_5$. Data are from Baxter (1972) and Table 1.

Intermediate Series basanites. As argued by Baxter (1976), the Younger Series characteristics could reflect either higher degrees of partial melting or low degrees of melting of a source already slightly depleted in the highly incompatible elements. Interestingly, the patterns for the Younger Series alkalic basalts (Fig. 3D) and subalkalic basalt C52 (Fig. 3E) all show peaks at Sr, in addition to Nb-Ta peaks. Several of these lavas appear to have lost variable amounts of K, U, and Rb; sample C52 also has a trough at P, which may be a result of alteration (its H$_2$O content is 1.43%). Two of the Younger Series samples (C29 in Fig. 3D, and C52 in Fig. 3E) have anomalously low Nb/Ta ratios (13.5 and 12.9, respectively, vs. the chondritic value of 17.6; e.g., Sun and McDonough, 1989); these two samples

appear to have suffered small amounts of Ta contamination during grinding in tungsten carbide.

Figure 4 shows the variation of several elements with MgO. The positive correlation between MgO and Ni (Fig. 4A) and MgO and Cr (Fig. 4B) are suggestive of olivine fractionation (with Cr entering chromite inclusions in olivine; e.g., Frey et al., 2000). Decreasing CaO/Al$_2$O$_3$ with decreasing MgO (Fig. 4C), on the other hand, is indicative of clinopyroxene fractionation. The marked inflections at about 10.5 and 6 wt% MgO may indicate that feldspar, with or without some other low-Ca phase, entered and then left (or played a smaller role in) the fractionating assemblage. For the Intermediate Series samples, including the basanites, the high CaO/Al$_2$O$_3$ may also reflect the retention of Al$_2$O$_3$ in

residual garnet at high pressure (see, e.g., Hirose, 1997). TiO_2 and P_2O_5 do not show meaningful correlations with MgO overall (Figs. 4D and 4E). However, for the Older Series, TiO_2 shows a good negative correlation with MgO, and the reversal of the TiO_2 trend at about 4 wt% MgO marks the onset of oxide fractionation. P_2O_5 also shows a good negative correlation with MgO for the Older Series, consistent with apatite fractionation, which is further supported by the appearance of apatite phenocrysts in the most evolved Older Series lavas (Baxter, 1972). The high Nb/Y and Tb/Yb values of the Intermediate Series basanites (Figs. 5A and 5B) are consistent with them being low-degree partial melts formed at depths where garnet is stable, inasmuch as Nb, Tb, and Th are incompatible in garnet, whereas Y and Yb behave compatibly in the presence of garnet (e.g., Arth, 1976).

Residual amphibole and phlogopite in the mantle source has been inferred for the rejuvenated-stage Honolulu Volcanics of the island of Oahu, Hawaii, and for some alkalic lavas of the Comores Archipelago, on the basis of depletion in K relative to other incompatible elements (Clague and Frey, 1982; Späth et al., 1996; Class and Goldstein, 1997; Class et al., 1998). In the presence of residual amphibole, K/Ce increases with increasing melt fraction, because the bulk solid-melt partition coefficient for K exceeds that of Ce (e.g., Francis and Ludden, 1995). No meaningful correlations between K/Ce and Ce, or Rb/Ce and Ce, are observed for our Mauritius samples (not shown). In part, this may be because of the small sample set for which Ce data are available; moreover, some of the samples have clearly suffered loss of K and Rb during alteration. In any case, the data provide no evidence for residual amphibole or phlogopite.

Nd-Sr Isotopes

Figure 6 compares the Nd-Sr isotopic ratios of the Mauritius lavas to those of mid-ocean ridge basalts (MORB) of the CIR and Carlsberg Ridge, basalts drilled during Leg 115 of the Ocean Drilling Program (Sites 707, 715, 713, and 706), basalts from Texaco drill site SM-1 on the Mascarene Plateau, and the Réunion lavas. Data for the Older Series lavas overlap, or lie very close to, the field defined by Réunion shield lavas. Together with similar Pb isotope characteristics (see below) and elemental characteristics, this result indicates closely similar mantle sources and petrogenetic evolution
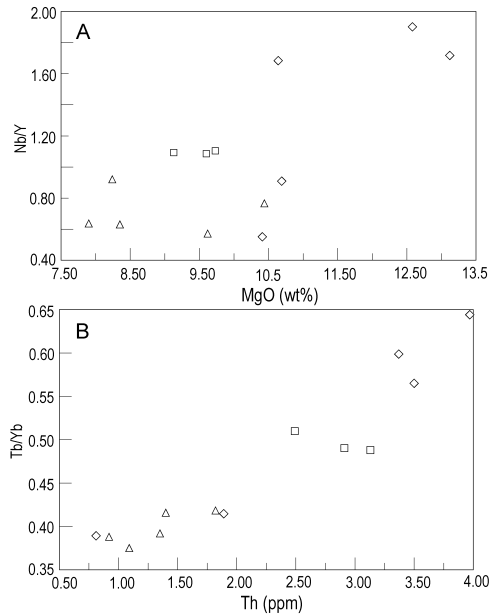

FIG. 5. Variation of (A) Nb/Y with MgO and (B) Tb/Yb with Th.

for the Mauritius Older Series and Réunion shield lavas (cf. Peng and Mahoney, 1995).

The Older Series lavas have $^{87}Sr/^{86}Sr$ ratios (0.70412–0.70433) consistently higher than those of the Intermediate and Younger Series (0.70369–0.70401), and the three series show a broad inverse relationship in $^{143}Nd/^{144}Nd$, with the Older Series lavas having consistently lower $^{143}Nd/^{144}Nd$ (0.512827–0.512853, ε_{Nd} = +3.6 to +4.1) than the Intermediate Series (0.512875–0.512899, ε_{Nd} +4.6 to +5.0) and Younger Series lavas (0.512874–0.512891, ε_{Nd} +4.6 to +4.9) (Fig. 6).[2] A similar inverse relationship is observed in many ocean island volcanoes, including Hawaiian volcanoes. Shield-building lavas of the Hawaiian chain have a wide range of isotopic compositions, but they are more radiogenic in Sr and less radiogenic in Nd than the post-shield and rejuvenated-stage lavas, which

---

[2]The sample A181, analyzed by Mahoney et al. (1989), has $^{143}Nd/^{144}Nd$ = 0.511876 relative to $^{143}Nd/^{144}Nd$ = 0.511845 for the La Jolla Nd standard, ε_{Nd} = +4.6, and $^{87}Sr/^{86}Sr$ = 0.70411. It is not clear whether this sample belongs to the Older or the Intermediate Series, inasmuch as it was collected near the boundary between the two types in a heavily forested area.
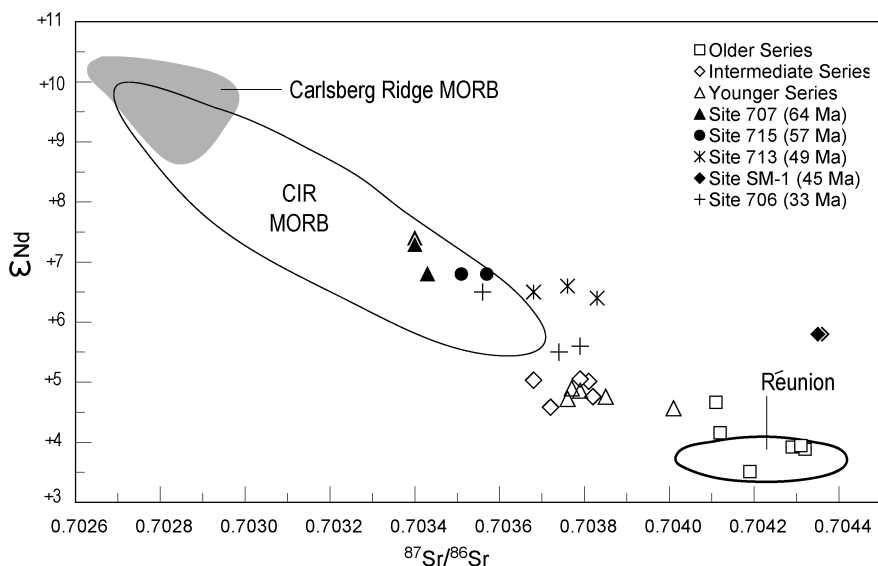
FIG. 6. Nd-Sr isotopic variations. All data are present-day values. Data sources for Mauritius are this study, Mahoney et al. (1989), and Peng and Mahoney (1995). Fields for CIR and Carlsberg Ridge MORB (Ito et al., 1987; Mahoney et al., 1989) and Réunion (Fisk et al., 1988) are shown for comparison, as are data for ODP Leg 115 and Texaco drill site SM-1 (White et al., 1990). Ages for the Leg 115 and SM-1 basalts are from Duncan and Hargraves (1990).

also are more alkalic than shield-stage lavas. These features of post-shield and rejuvenated-stage volcanism have been interpreted as indicating either low-degree melting or recent (<400 Ma) mantle metasomatism involving material from comparatively MORB-like mantle (e.g., Clague and Frey, 1982; Stille et al., 1983; Chen and Frey, 1983, 1985; Feigenson, 1984; Roden et al., 1984; Clague and Dalrymple, 1988; Maaløe et al., 1992; Reiners and Nelson, 1998; Frey et al., 2000).

Nd and Sr isotopic ratios of the Intermediate and Younger Series Mauritius lavas overlap, and cluster in a small area (consistent with a common, relatively homogeneous mantle source for both) between the Older Series and Réunion values and the CIR MORB field in Figure 6. The Intermediate and Younger Series may therefore represent melts of a mixed mantle source (cf. Mahoney et al., 1989). Their relative closeness to CIR MORB isotopic compositions is also consistent with their helium isotopic ratios. Hanyu et al. (2001) reported that $^3He/^4He$ ratios of both volcanoes on Réunion are uniform (12-13.5 R_a, where R_a is the atmospheric $^3He/^4He$ ratio) regardless of ^4He content and sample age, and that values for the Mauritius Older Series lavas are very similar, around 11.5 R_a. In contrast, the Intermedi-

ate and Younger Series (and Rodrigues) lavas have $^3He/^4He$ (6.5-8.4 R_a) similar to Indian MORB ratios.

The Leg 115 and SM-1 basalts have higher ε_{Nd} values than the Intermediate and Younger Series lavas, within or close to the CIR MORB range (Fig. 6). Values for the youngest drill site, Site 706 (33 Ma), are closest to those of Mauritius and Réunion. White et al. (1990) argued that, as a group, the ε_{Nd} values of the Leg 115 basalts and Réunion showed an overall decrease, and $^{87}Sr/^{86}Sr$ a rough increase, with decreasing age. Within the framework of the mantle plume model for ocean island volcanism (e.g., Richards et al., 1989), they interpreted this trend as reflecting progressively decreasing entrainment of asthenospheric (MORB-source) mantle by the upwelling plume. Noting the relatively high Sr isotope values of several of the drilled samples, they concluded that $^{87}Sr/^{86}Sr$ also may have been variably increased by seawater alteration. Nd isotopic ratios are not affected by low to moderate levels of seawater alteration, however, and do not appear to vary systematically with age, except that lavas of the two oldest sites (at 64 and 57 Ma) have slightly higher ε_{Nd} than those of the three younger sites (49–33 Ma). In any case, it is not clear that the drill sites recovered shield-stage lavas. Given that the
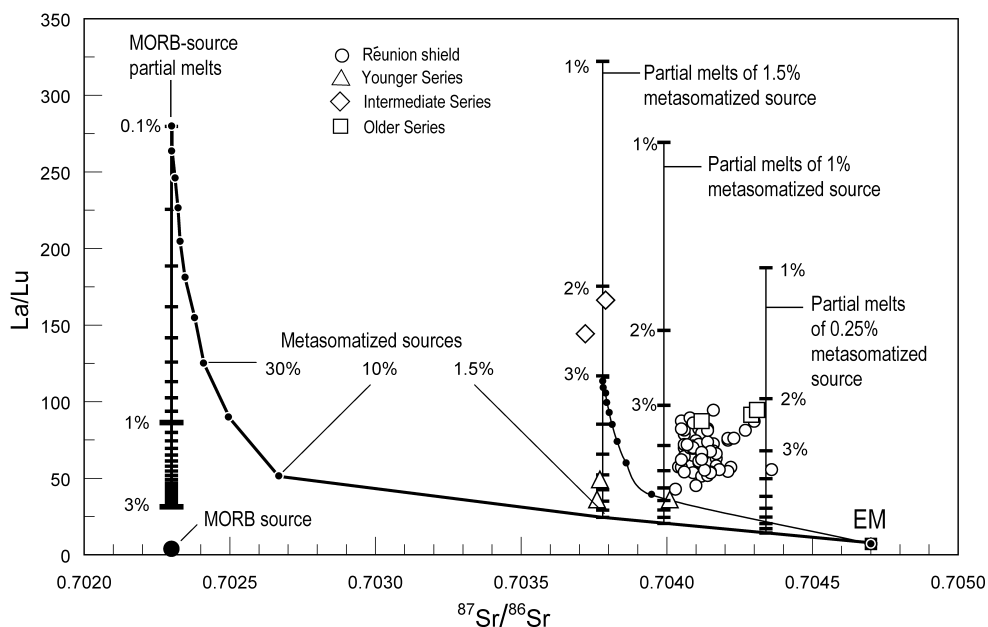
FIG. 7. Illustration of MORB-source and EM partial melting and mixing model for the Mauritius lavas. Data for Réunion shield lavas are also shown (from Fisk et al., 1988; Albarède et al., 1997). The K_d values used are from Reiners and Nelson (1998): for La, olivine/melt = 0.00045, orthopyroxene/melt = 0.00125, clinopyroxene/melt = 0.037, and garnet/melt = 0.007; for Lu, olivine/melt = 0.00315, orthopyroxene/melt = 0.049, clinopyroxene/melt = 0.235, and garnet/melt = 5.6; for Sr, olivine/melt = 0.0015, orthopyroxene/melt = 0.016, clinopyroxene/melt = 0.1, and garnet/melt = 0.008.

post-shield Intermediate and Younger Series lavas of Mauritius are more MORB-like in Nd-Sr isotopic characteristics than the shield-stage Older Series, it is possible, perhaps likely, that the drill-site lavas represent post-shield volcanism and that shield-stage lavas were not penetrated during drilling.

A Partial Melting–Mixing Model

Chen and Frey (1983, 1985) explained the transition from shield-stage to post-shield volcanism in the Haleakala Volcano of Maui, Hawaii, with a mixing model in which the proportion of MORB-source mantle to plume mantle increases after the end of the shield stage. Roden et al. (1984) invoked solid-melt mixing, and interpreted the rejuvenated-stage Honolulu Volcanics of Oahu as products of mixing between melts of a MORB-type mantle source and the plume. They estimated that the MORB-type mantle melted to ~0.3%, and that the mixture contained ~2.5% of these partial melts. Others have proposed mixing of relatively high-degree plume-derived melts with smaller-degree MORB-source melts (e.g., Feigenson, 1984; Clague and Dalrymple, 1988). Whatever the source of the low-ε_{Nd}, high-$^{87}Sr/^{86}Sr$ mantle component (plume or otherwise) and the MORB-like mantle, there is consensus that *mixing* of mantle sources and/or melts is required to explain the inverse relationships in isotopic ratios and incompatible element abundances between Hawaiian shield and post-shield or rejuvenated-stage lavas.

In Figure 7, we summarize a petrogenetic model for the Mauritius lavas, which is a modified version of that used by Chen and Frey (1983). The model invokes two mixing end members, one of which is MORB-source mantle and the other a mantle source (EM) with bulk-Earth–like Sr and Nd isotope ratios. The physical nature of these sources can have variable interpretations. For example, in the mantle plume model (e.g., Richards et al., 1989; Campbell and Griffiths, 1990), EM can represent an upwelling deep mantle plume and the MORB source can represent mantle entrained by the plume or it can be

lower oceanic lithosphere under an island. In non-plume models (e.g., Smith, 1993; Anderson, 1995, 1996; Smith and Lewis, 1999), EM can represent detached continental lithospheric mantle or a shallow "perisphere," whereas the MORB source can be the oceanic lithosphere or sub-perispheric convecting mantle. Our model postulates metasomatism of EM by low-degree partial melts of the MORB source.

To a first order, the Mauritius and Réunion lavas can be explained as partial melts of variably metasomatized EM sources, or as mixtures of these partial melts from the MORB source and EM. Figure 7 illustrates the model in terms of La/Lu and $^{87}Sr/^{86}Sr$, parameters used by Reiners and Nelson (1998) to model the Koloa Volcanics of Kauai, Hawaii. As assumed by Reiners and Nelson (1998), the MORB source has the following composition: La = 0.206 ppm, Lu = 0.054 ppm, Sr = 13.2 ppm, and $^{87}Sr/^{86}Sr$ = 0.70230. EM has the following composition: La = 0.71 ppm, Lu = 0.1 ppm, Sr = 23.7 ppm, and $^{87}Sr/^{86}Sr$ = 0.70470. Non-modal, equilibrium (batch) melting of the MORB source mantle was assumed. The initial mode of the MORB source was taken to be 65% olivine, 24% orthopyroxene, 6% clinopyroxene, and 5% garnet, and the melts to correspond to 10% olivine, 10% orthopyroxene, 40% clinopyroxene, and 40% garnet. Partition coefficient (K_d) values used for La, Lu, and Sr are given in Figure 7.

The constant $^{87}Sr/^{86}Sr$ vertical line above the MORB source point shows how La/Lu varies as a function of melt fraction (F) for 0.1–3% melting of the MORB source. A 0.1% MORB-source partial melt has La = 49.3 ppm, Lu = 0.176 ppm, and Sr = 1086 ppm. The large hyperbola shows various binary mixtures of this 0.1% partial melt and EM (dots mark 10% increments). Different points on this curve therefore represent EM metasomatized to varying amounts by a 0.1% MORB-source melt. Five of these metasomatized EM sources (30%, 10%, 1.5%, 1%, and 0.25%) are indicated by labels. The 1.5% metasomatized source, for example, has La = 1.44 ppm, Lu = 0.10 ppm, Sr = 39.6 ppm, and $^{87}Sr/^{86}Sr$ = 0.70378. The constant $^{87}Sr/^{86}Sr$ vertical line rising from it shows the compositions of various partial melts (1–8%) of this source. Data for four Mauritius Younger and Intermediate Series samples plot near this line; the two Intermediate Series data points (for basanites B5 and B33) can be interpreted as representing ~2.5% partial melts of the 1.5% metasomatized source, whereas the two Younger

Series samples (basalts C29 and C52) would represent larger amounts of melting (6.5–8%). On the other hand, the data point for Younger Series alkalic basalt C20 (with higher $^{87}Sr/^{86}Sr$ = 0.70401) is consistent with 7% melting of a 1% metasomatized source. Alternatively, this lava composition can be interpreted as a second-stage mixture lying on a mixing curve between a 3% partial melt of the 1.5% metasomatized source and pure EM, the proportion of the 3% partial melt in the mixture being ~8%.

Figure 7 also shows partial melts of a 0.25% metasomatized EM source, with La = 0.83 ppm, Lu = 0.10 ppm, Sr = 26.4 ppm, and $^{87}Sr/^{86}Sr$ = 0.70434. Data for the Older Series and Réunion shield lavas are completely bounded by the lines representing melting of 1% and 0.25% metasomatized sources, at melt fractions between 2 and 6%. All Older Series and Réunion lavas can therefore be interpreted as 2–6% partial melts of an EM source that is 1% to 0.25% metasomatized by a 0.1% partial melt of the MORB source. Interpretation of the Older Series and Réunion lavas as second-stage mixtures is also possible. All the data are bounded by the mixing curves between a 3% partial melt of the 1.5% metasomatized source and EM (Fig. 7), and a 0.1% partial melt of the 1.5% metasomatized source and EM (not shown). Thus, the shield lavas can also be interpreted as blends of: (1) EM, and (2) variable but low-degree (0.1–3%) partial melts of a source that itself is a 1.5:98.5 mixture of a 0.1% partial melt of a MORB source and EM. Lacking further evidence, we prefer to interpret the Mauritius (and Réunion) shield lavas as simple partial melts of variable (1.5%–0.25%) first-stage mixtures of EM and a 0.1% MORB-source partial melt.

Pb Isotopes

As with Nd and Sr isotopes, the Pb isotope ratios of the Older Series lavas closely resemble those of Réunion shield lavas, although covering a slightly wider range than yet measured for Réunion (the Réunion field in Figure 8 encloses data for seven samples). Very small differences in $^{207}Pb/^{204}Pb$ (<0.01; Fig. 8D) between the Older Series and Réunion data may simply represent inter-laboratory bias; indeed, the differences are within analytical error for Peng and Mahoney's (1995) two earlier Older Series analyses that were not made by the double-spike method. The Pb isotopic ratios of the three Intermediate Series lavas have a significantly greater range ($^{206}Pb/^{204}Pb$ varies from 18.634 to
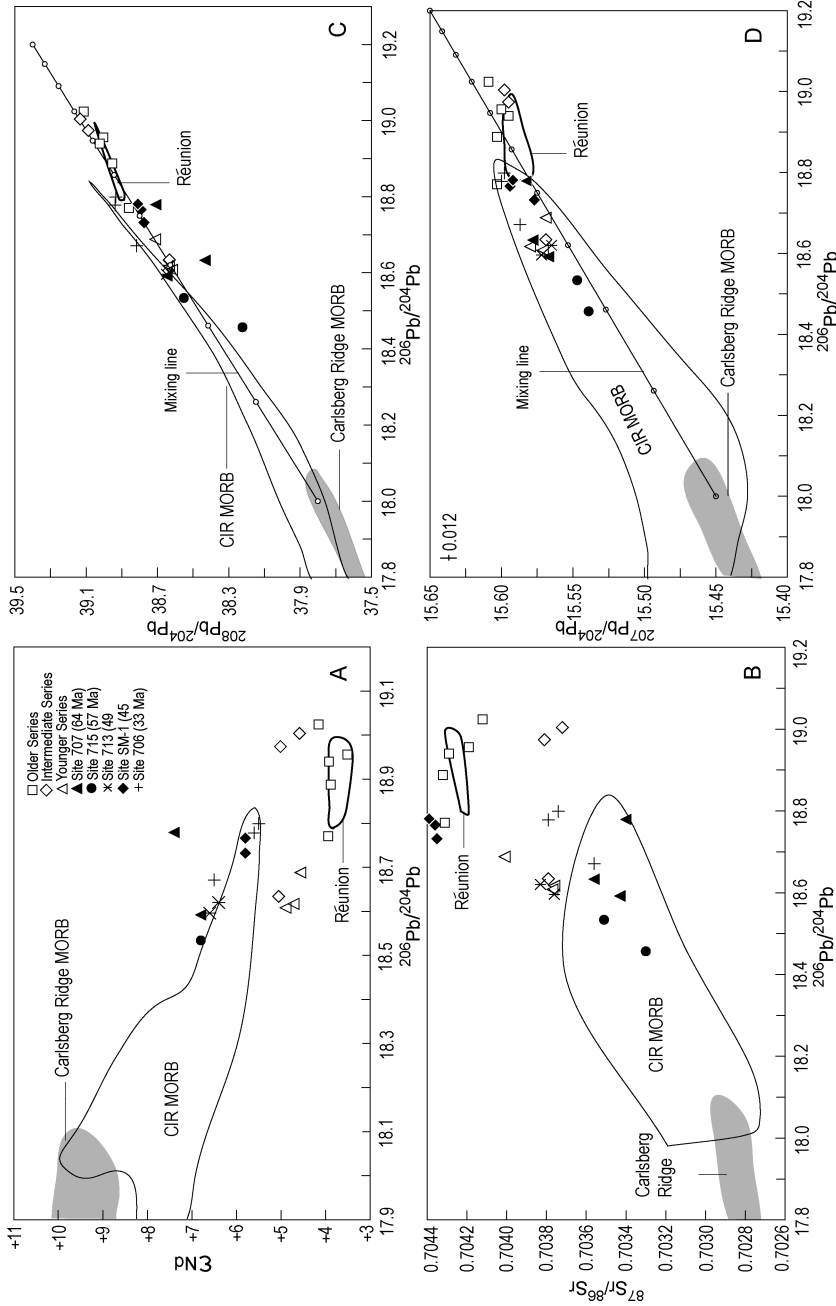
FIG. 8. Nd-Sr-Pb isotopic variations in the Mauritius lavas. A. ε_{Nd} vs. $^{206}Pb/^{204}Pb$. B. $^{87}Sr/^{86}Sr$ vs. $^{206}Pb/^{204}Pb$. C. $^{208}Pb/^{204}Pb$ vs. $^{206}Pb/^{204}Pb$. D. $^{207}Pb/^{204}Pb$ vs. $^{206}Pb/^{204}Pb$. Data sources are the same as those used in Figure 6, plus W. M. White (unpubl.). The lines in panels C and D show simple mixing between two hypothetical end members, one similar to Indian MORB mantle (with $Pb = 0.04$ ppm, $^{206}Pb/^{204}Pb = 18.000$, $^{207}Pb/^{204}Pb = 15.45$, $^{208}Pb/^{204}Pb = 37.800$) and the other with much higher Pb isotopic ratios ($^{206}Pb/^{204}Pb = 19.200$, $^{207}Pb/^{204}Pb = 15.65$, $^{208}Pb/^{204}Pb = 39.400$) and $Pb = 0.1$ ppm. Small open circles on the mixing lines mark 10% increments. Error bar in panel D shows typical error for non-double-spike ratios (± 0.012) of Peng and Mahoney (1995).
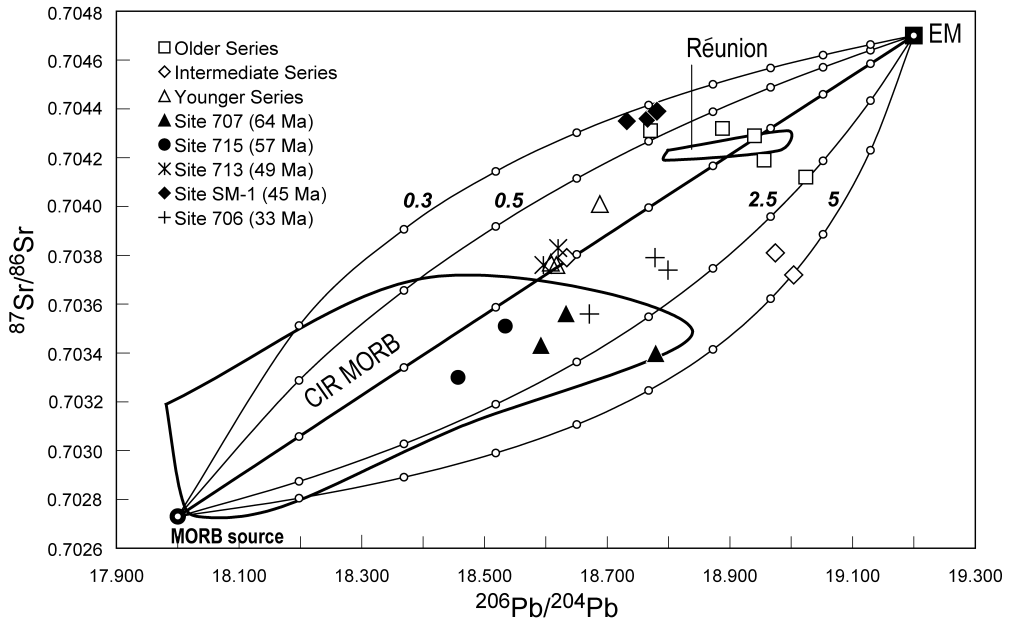
FIG. 9. Small open circles on the mixing curves mark 10% mixing increments, and the ratio of the Sr/Pb values of the two mixing end members is shown beside each curve. For ratios of 5, 2.5, 0.5, and 0.3, the required Sr concentrations in the "MORB source" are 66.8 ppm, 33.4 ppm, 6.68 ppm, and 4.00 ppm, respectively, assuming the Pb concentration of the MORB source is constant at 0.04 ppm, and that the Pb and Sr concentrations of EM are constant, at 0.071 and 23.7 ppm, respectively. Data sources are the same as those in Figure 8.

19.004), from values lower than any measured for the Older Series to almost as high as the highest Older Series value. In contrast, the three Younger Series samples that we analyzed have relatively low Pb isotope ratios that vary only slightly ($^{206}Pb/^{204}Pb$ = 18.608 to 18.688). If the Intermediate and Younger Series lavas were derived from a common mantle source rather homogeneous in Nd and Sr isotopes, it would seem to have possessed considerable Pb isotopic heterogeneity. In the previous section, we assumed that the two mantle end-members each had a single, fixed isotopic and elemental composition (i.e., each could be represented as a point on chemical and isotopic diagrams); however, the range exhibited by the Mauritius, Réunion, and drill-site lavas in ε_{Nd}-$^{87}Sr/^{86}Sr$-$^{206}Pb/^{204}Pb$ space (Figs. 8A and 8B) indicates that one or both end-members would have to have at least a modest range of compositions. The same can be seen from plots of $^{208}Pb/^{204}Pb$ vs. $^{206}Pb/^{204}Pb$ (Fig. 8C) and $^{207}Pb/^{204}Pb$ vs. $^{206}Pb/^{204}Pb$ (Fig. 3D).

Assuming for the moment that each of the two end-members were isotopically homogeneous, however, the heavy line in Figure 9 is a mixing curve between a MORB source (assumed to have Sr = 13.2 ppm, Pb = 0.04 ppm, $^{87}Sr/^{86}Sr$ = 0.70273, $^{206}Pb/^{204}Pb$ = 18.000) and EM (assumed to have Sr = 23.7 ppm, Pb = 0.071 ppm, $^{87}Sr/^{86}Sr$ = 0.70470, $^{206}Pb/^{204}Pb$ = 19.200). Elemental abundances in the two end-members are based on Sun and McDonough (1989), and EM is similar to their estimate of primitive mantle, but the EM value of 19.200 for $^{206}Pb/^{204}Pb$ is arbitrarily chosen to exceed the highest value measured for the Mauritius samples. This value is higher than estimates for primitive mantle but close to that of the postulated "Common" or "C" mantle component (Hanan and Graham, 1996). The chosen $^{87}Sr/^{86}Sr$ and $^{206}Pb/^{204}Pb$ ratios of the MORB source end-member are nearly identical with those of CIR MORB sample ANTP131-14 (ε_{Nd} = +10.0, $^{87}Sr/^{86}Sr$ = 0.70273, $^{206}Pb/^{204}Pb$ = 18.033; Mahoney et al., 1989). The heavy mixing curve is nearly straight, inasmuch as Sr/Pb is about equal in the two end-members. For mixing curves that encompass the total range of compositions observed, the Sr/Pb ratios of the two end-members must be significantly different. Four other curves in Figure 9 represent mixtures assuming that Sr/Pb in the MORB source

varies from 5 times to 0.3 times the Sr/Pb value in EM; this range is necessary for the mixing curves to encompass the Sr-Pb isotopic range exhibited by the Mauritius, Réunion, and drill-site samples. Isotopically MORB-like end-members with higher Sr/Pb than EM could represent appropriately plagioclase-enriched cumulate rocks within the oceanic lithosphere (see e.g., Frey et al., 2002), whereas MORB-like end-members with lower Sr/Pb than EM could be the complementary plagioclase-poor rocks (olivine-clinopyroxene cumulates?). However, such an explanation appears untenable because, although undoubtedly modified somewhat by crystal fractionation, the measured Sr/Pb values among the Mauritius samples vary by only a factor of 3.2 (range of Sr/Pb is 145 to 466), and do not correlate with $^{87}Sr/^{86}Sr$. Thus, end members that are isotopically somewhat heterogeneous again appear to be required.

Note that the Older Series, Intermediate Series, and Réunion arrays in Figure 9 trend across mixing curves. This behavior can be explained if one or both of the two end members are isotopically somewhat heterogeneous in Pb isotopes. Alternatively, the range in $^{206}Pb/^{204}Pb$ at similar Sr and Nd isotope ratios could partly represent radiogenic ingrowth since the mixing event, assuming that somewhat variable U/Pb ratios were produced in different parts of the metasomatized source. The $^{206}Pb/^{204}Pb$ ratio tends to evolve much faster than $^{87}Sr/^{86}Sr$ and ε_{Nd}, because parent-daughter ratios in the ^{238}U-^{206}Pb system tend to be large (the range in our samples is 2.58 [for B18] to 28.7 [for B34]) and the half-life of ^{238}U is much shorter than those of ^{87}Rb and ^{147}Sm (by a factor of more than 10 and 23, respectively). For example, a relatively small difference in source $^{238}U/^{204}Pb$ of only 5 will lead to a difference in $^{206}Pb/^{204}Pb$ of 0.25, the maximum range measured for the Older Series, in 314 m.y. Over the same period, the maximum differences observed in $^{147}Sm/^{144}Nd$ and $^{87}Rb/^{86}Sr$ for the Older Series lavas would lead to Nd and Sr isotopic differences of only 0.3 ε_{Nd} units and 0.00022, respectively. Unfortunately, a direct test of this possibility is not possible, because magmatic and alteration processes have variably modified the source-derived $^{238}U/^{204}Pb$ signal in the Mauritius samples. However, general support is provided by the very small observed range in $^{207}Pb/^{204}Pb$ relative to that in $^{206}Pb/^{204}Pb$ for the Older Series samples. This variation in $^{207}Pb/^{204}Pb$ (0.014) is effectively the same as the largest analytical uncertainties on the data (i.e., ±0.012 on Peng and Mahoney's [1995] data); the Réunion data also define a rather flat field (Fig. 8D). This feature is qualitatively consistent with radiogenic ingrowth of Pb following a metasomatic event in the not too distant past; for example, the difference in $^{238}U/^{204}Pb$ of 5 used in the above example corresponds to a $^{235}U/^{204}Pb$ difference of 0.036, which would lead in 314 m.y. to a difference of only 0.013 in $^{207}Pb/^{204}Pb$.

Conclusions

The volcanic, petrological, and geochemical evolution of Mauritius is similar to that of many ocean islands worldwide. The Older Series lavas (shield-building stage) of Mauritius are closely similar to those of Réunion Island in major- and trace-element and Nd-Sr-Pb isotopic compositions. The post-shield Intermediate and Younger Series lavas have overlapping Nd-Sr isotopic compositions that are slightly more MORB-like than those of the Older Series; their Pb isotope ratios also extend to more MORB-like values, but Pb isotope ratios for the Intermediate Series cover nearly the full range observed for all three series. Most Intermediate Series lavas are strongly enriched in highly incompatible elements relative to moderately incompatible ones, but the Younger Series lavas display much less relative enrichment and have low concentrations of incompatible elements. Post-shield lavas with incompatible element enrichment deriving from mantle sources with long-term relative depletion in incompatible elements (as reflected in isotopic ratios) have been observed in ocean islands worldwide (e.g., Hawaii). A partial melting and mixing model for the Mauritius lavas relates them to various extents of partial melting and mixing between a MORB source and a source (EM) with bulk-Earth–like elemental and Nd-Sr isotopic characteristics and a "C"-like Pb isotopic signature. Many characteristics of the Mauritius and Réunion lavas can be explained if these lavas represent 2–8% partial melts of an EM source that had been 1.5–0.25% metasomatized by a 0.1% MORB-source melt. However, some Pb isotope heterogeneity is required in the end-members, and/or the Pb isotope variation reflects variable radiogenic ingrowth since the metasomatic event, which must have occurred within the last few hundred million years.

Acknowledgments

Young Investigator award at the University of Hawaii. We thank Denys VonderHaar for valuable assistance in the ICP-MS lab, and Bill White for use of his unpublished data for Réunion.

REFERENCES

Albarède, F., and Tamagnan, V., 1988, Modelling the recent geochemical evolution of the Piton de la Fournaise volcano, Réunion Island: Journal of Petrology, v. 29, p. 997–1030.

Albarède, F., Luais, B., Fitton, J. G., Semet, M., Kaminski, E., Upton, B. G. J., Bachèlery, P., and Cheminée, J.-L., 1997, The geochemical regimes of Piton de la Fournaise volcano (Réunion) during the last 530,000 years: Journal of Petrology, v. 38, p. 171–201.

Anderson, D. L., 1995, Lithosphere, asthenosphere, and perisphere: Reviews of Geophysics, v. 33, p. 125–149.

———, 1996, Enriched asthenosphere and depleted plumes: International Geology Review, v. 38, p. 1–21.

Arth, J. G., 1976, Behavior of trace elements during magmatic processes—a summary of theoretical models and their applications: Journal of Research of the United States Geological Survey, v. 4, p. 41–47.

Bachèlery, P., Blum, P. A., Cheminée, J. L., Chevallier, L., Gaulon, R., Girardin, N., Jaupart, C., Lalanne, F., Le Mouel, J. L., Ruegg, J. C., and Vincent, P., 1982, Eruption at Le Piton de la Fournaise Volcano on 3 February 1981: Nature, v. 297, p. 395–397.

Baxter, A. N., 1972, Magmatic evolution of Mauritius, western Indian Ocean: Unpubl. Ph.D. dissertation, University of Edinburgh, 177 pp.

———, 1975a, Petrology of the Older Series lavas from Mauritius, Indian Ocean: Geological Society of America Bulletin, v. 86, p. 1449–1458.

———, 1975b, K/Rb ratios in some volcanic rocks from Mauritius, Indian Ocean: Geochimica et Cosmochimica Acta, v. 39, p. 1573–1576.

———, 1976, Geochemistry and petrogenesis of primitive alkali basalt from Mauritius, Indian Ocean: Geological Society of America Bulletin, v. 87, p. 1028–1034.

Baxter, A. N., Upton, B. G. J., and White, W. M., 1985, Petrology and geochemistry of Rodrigues Island, Indian Ocean: Contributions to Mineralogy and Petrology, v. 89, p. 90–101.

Campbell, I. H., and Griffiths, R. W., 1990, Implications of mantle plume structure for the evolution of flood basalts: Earth and Planetary Science Letters, v. 99, p. 79–93.

Chen, C.-Y., and Frey, F. A., 1983, Origin of Hawaiian tholeiite and alkalic basalt: Nature, v. 302, p. 785–789.

———, 1985, Trace element and isotopic geochemistry of lavas from Haleakala volcano, East Maui, Hawaii:

Implications for the origin of Hawaiian lavas: Journal of Geophysical Research, v. 90, p. 8743–8768.

Clague, D. A., 1987, Hawaiian alkaline volcanism, *in* Fitton, J. G., and Upton, B. G. J., eds., Alkaline igneous rocks: Geological Society of London, Special Publications, v. 30, p. 227–252.

Clague, D. A., and Dalrymple, G. B., 1988, Age and petrology of alkalic postshield and rejuvenated-stage lava from Kauai, Hawaii: Contributions to Mineralogy and Petrology, v. 99, p. 202–218.

Clague, D. A., and Frey, F. A., 1982, Petrology and trace element geochemistry of the Honolulu volcanics, Oahu: Implications for the oceanic mantle below Hawaii: Journal of Petrology, v. 23, p. 447–504.

Class, C., and Goldstein, S. L., 1997, Plume-lithosphere interactions in the ocean basins: Constraints from source mineralogy: Earth and Planetary Science Letters, v. 150, p. 145–260.

Class, C., Goldstein, S. L., Altherr, R., and Bachèlery, P., 1998, The process of plume-lithosphere interactions in the ocean basins—the case of Grande Comore: Journal of Petrology, v. 39, p. 881–903.

Duncan, R. A., 1990, The volcanic record of the Réunion hotspot, *in* Duncan, R. A., Backman, J., Peterson, L. C., et al., eds., Proceedings of the Ocean Drilling Program, Scientific Results, v. 115, p. 3–10.

Duncan, R. A., and Hargraves, R. B., 1990, $^{40}Ar/^{39}Ar$ geochronology of basement rocks from the Mascarene Plateau, the Chagos Bank, and the Maldives Ridge, *in* Proceedings of the Ocean Drilling Program, Scientific Results, v. 115, p. 43–51.

Feigenson, M. D., 1984, Geochemistry of Kauai volcanics and a mixing model for the origin of Hawaiian alkalic basalts: Contributions to Mineralogy and Petrology, v. 87, p. 109–119.

Fisher, R. L., Johnson, G. L., and Heezen, B. C., 1967, Mascarene Plateau, western Indian Ocean: Geological Society of America Bulletin, v. 78, p. 1247–1266.

Fisher, R. L., Sclater, J. G., and McKenzie, D. P., 1971, Evolution of the Central Indian Ridge, Western Indian Ocean: Geological Society of America Bulletin, v. 82, p. 553–562.

Fisk, M. R., Upton, B. G. J., and Ford, C. E., 1988, Geochemical and experimental study of the genesis of magmas of Réunion Island, Indian Ocean: Journal of Geophysical Research, v. 93, p. 4933–4950.

Francis, D., and Ludden, J., 1995, The signature of amphibole in mafic alkaline lavas: A study in the Northern Canadian Cordillera: Journal of Petrology, v. 36, p. 1171–1191.

Frey, F. A., Clague, D., Mahoney, J. J., and Sinton, J. M., 2000, Volcanism at the edge of the Hawaiian plume: Petrogenesis of submarine alkalic lavas from the North Arch volcanic field: Journal of Petrology, v. 41, p. 667–691.

Frey, F. A., Weis, D., Borisova, A. Yu., and Xu, G., 2002, Involvement of continental crust in the formation of the

Cretaceous Kerguelen plateau: New perspectives from ODP Leg 120 sites: Journal of Petrology, v. 43, p. 1207–1239.

Galer, S. J. G., 1999, Optimal double and triple spiking for high precision lead isotopic measurement: Chemical Geology, v. 157, p. 255–274.

Gillot, P.-Y., and Nativel, P., 1989, Eruptive history of the Piton de la Fournaise volcano, Réunion Island, Indian Ocean: Journal of Volcanology and Geothermal Research, v. 36, p. 53–65.

Govindaraju, K., 1989, Compilation of working values and sample descriptions for 272 geostandards: Geostandards Newsletter, v. 13, p. 1–113.

Hanan, B. B., and Graham, D. W., 1996, Lead and helium isotope evidence from oceanic basalts for a common deep source of mantle plumes: Science, v. 272, p. 991–995.

Hanyu, T., Dunai, T. J., Davies, G. R., Kaneoka, I., Nohda, S., and Uto, K., 2001, Noble gas study of the Réunion hotspot: Evidence for distinct less-degassed mantle sources: Earth and Planetary Science Letters, v. 193, p. 83–98.

Hirose, K., 1997, Partial melt compositions of carbonated peridotite at 3 Gpa and role of CO_2 in alkali-basalt magma generation: Geophysical Research Letters, v. 24, p. 2837–2840.

Irvine, T. N., and Baragar, W. R. A., 1971, A guide to the chemical classification of the common volcanic rocks: Canadian Journal of Earth Sciences, v. 8, p. 523–548.

Ito, E., White, W. M., and Göpel, C., 1987, The O, Sr, Nd, and Pb isotope geochemistry of MORB: Chemical Geology, v. 62, p. 157-176.

Jain, J. C., and Neal, C. R., 1996, Report of the ICP-MS facility, 1993-1996: South Bend, IN: Notre Dame University, Open File Report, 30 p.

Le Bas, M. J., Le Maitre, R. W., Streckeisen, A., and Zanettin, B., 1986, A chemical classification of volcanic rocks on the total alkali-silica diagram: Journal of Petrology, v. 27, p. 745–750.

Maaløe, S., James, D., Smedley, P., Petersen, S., and Garmann, L. B., 1992, The Koloa Volcanic suite of Kauai, Hawaii: Journal of Petrology, v. 33, p. 761–784.

Macdonald, G. A., 1968, Composition and origin of Hawaiian lavas, *in* Coats, R. E., Hay, R. L., and Anderson, C. A., eds., Studies in volcanology: Geological Society of America Memoirs, v. 116, p. 477–522.

Macdonald, G. A., and Katsura, T., 1964, Chemical composition of Hawaiian lavas: Journal of Petrology, v. 5, p. 82–133.

Mahoney, J. J., Duncan, R. A., Khan, W., Gnos, E., and McCormick, G. R., 2002, Cretaceous volcanic rocks of the South Tethyan suture zone, Pakistan: Implications for the Réunion hotspot and the Deccan traps: Earth and Planetary Science Letters, v. 203, p. 295–310.

Mahoney, J. J., Natland, J. H., White, W. M., Poreda, R., Bloomer, S. H., Fisher, R. L., and Baxter, A. N., 1989,

Isotopic and geochemical provinces of the western Indian ocean spreading centers: Journal of Geophysical Research, v. 94, p. 4033–4052.

Mahoney, J. J., Nicollet, C., and Dupuy, C., 1991, Madagascar basalts: Tracking oceanic and continental sources: Earth and Planetary Science Letters, v. 104, p. 350–363.

McDougall, I., 1971, The geochronology and evolution of the young oceanic island of Réunion, Indian Ocean: Geochimica et Cosmochimica Acta, v. 35, 261–270.

McDougall, I., and Chamalaun, F. G., 1969, Isotopic dating and geomagnetic polarity studies on volcanic rocks from Mauritius, Indian Ocean: Geological Society of America Bulletin, v. 80, p. 1419–1442.

McDougall, I., Upton, B. G. J., and Wadsworth, W. J., 1965, A geological reconnaissance of Rodrigues Island, Indian Ocean: Nature, v. 206, p. 26–27.

Morgan, W. J., 1981, Hotspot tracks and the opening of the Atlantic and Indian Oceans, *in* Emiliani, C., ed., The Sea: New York, NY, John Wiley, v. 7, p. 443–487.

O'Hara, M. J., Richardson, S. W., and Wilson, G., 1971, Garnet-peridotite stability and occurrence in the crust and mantle: Contributions to Mineralogy and Petrology, v. 32, p. 48–68.

Peng, Z. X., and Mahoney, J. J., 1995, Drillhole lavas from the northwestern Deccan Traps, and the evolution of Réunion hotspot mantle: Earth and Planetary Science Letters, v. 134, p. 169–185.

Potts, P. J., Tindle, A. G., and Webb, P. C., 1992, Geochemical reference material compositions: Rocks, minerals, sediments, soils, carbonates, refractories and ores used in research and industry: Caithness, UK, Whittles Publishing.

Reiners, P. W., and Nelson, B. K., 1998, Temporal-compositional-isotopic trends in rejuvenated stage magmas of Kauai, Hawaii, and implications for mantle melting process: Geochimica et Cosmochimica Acta, v. 62, p. 2347–2368.

Richards, M. A., Duncan, R. A., and Courtillot, V. E., 1989, Flood basalts and hotspot tracks: Plume heads and tails: Science, v. 246, p. 103–107.

Roden, M. F., Frey, F. A., and Clague, D. A., 1984, Geochemistry of tholeiitic and alkalic lavas from the Koolau Range, Oahu, Hawaii: Implications for Hawaiian volcanism: Earth and Planetary Science Letters, v. 69, p. 141–158.

Smith, A. D., 1993, The continental mantle as a source for hotspot volcanism: Terra Nova, v. 5, p. 452–460.

Smith, A. D., and Lewis, C., 1999, The planet beyond the plume hypothesis: Earth-Science Reviews, v. 42, p. 135–182.

Späth, A., le Roex, A. P., and Duncan, R. A., 1996, The geochemistry of lavas from the Comores Archipelago, western Indian Ocean: petrogenesis and mantle source region characteristics: Journal of Petrology, v. 37, p. 961–991.

Staudacher, T., Sarda, P., and Allègre, C. J., 1990, Noble gas systematics of Réunion Island, Indian Ocean: Chemical Geology, v. 89, p. 1–17.

Stearns, H. T., 1940, Four-phase volcanism in Hawaii: Geological Society of America Bulletin, v. 51, p. 1947–1948.

Stille, P., Unruh, D. M., and Tatsumoto, M., 1983, Pb, Sr, Nd, and Hf isotopic evidence of multiple sources for Oahu, Hawaii basalts: Nature, v. 304, p. 25–29.

Sun, S.-s., and McDonough, W. F., 1989, Chemical and isotopic systematics of oceanic basalts: Implications for mantle composition and processes, *in* Saunders, A. D., and Norry, M. J., eds., Magmatism in the ocean basins: Geological Society of London, Special Publications, v. 42, p. 313–345.

Verma, S. P., Torres-Alvarado, I. S., and Sotelo-Rodríguez, Z., 2002, SINCLAS: Standard igneous norm and volcanic rock classification system: Computers and Geosciences, v. 28, p. 711–715.

White, W. M., Cheatham, M. M., and Duncan, R. A., 1990, Isotope geochemistry of Leg 115 basalts and inferences on the history of the Réunion mantle plume, *in* Duncan, R. A., Backman, J., Peterson, L. C., et al., eds., Proceedings of the Ocean Drilling Program, Scientific Results, v. 115, p. 53–61.